

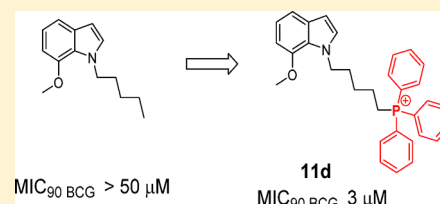
## Indolylalkyltriphenylphosphonium Analogues Are Membrane-Depolarizing Mycobactericidal Agents

Ming Li,<sup>†,⊥</sup> Samuel A. Nyantakyi,<sup>‡,⊥</sup> Pooja Gopal,<sup>†</sup> Dinah binte Aziz,<sup>†</sup> Thomas Dick,<sup>§,||</sup> and Mei-Lin Go<sup>\*,‡,⊥</sup><sup>†</sup>Department of Medicine and <sup>§</sup>Department of Microbiology and Immunology, Yong Loo Lin School of Medicine, National University of Singapore, Singapore 119228<sup>‡</sup>Department of Pharmacy, Faculty of Science, National University of Singapore, Singapore 117543<sup>||</sup>Public Health Research Institute, New Jersey Medical School, Rutgers, The State University of New Jersey, Newark, New Jersey 07103, United States

## Supporting Information

**ABSTRACT:** Agents that selectively target the mycobacterial membrane could potentially shorten treatment time for tuberculosis, reduce relapse, and curtail emergence of resistant strains. The lipophilicity and extensive charge-delocalized state of the triphenylphosphonium cation strongly favor accumulation within bacterial membranes. Here, we explored the antimycobacterial activities and membrane-targeting properties of indolylalkyltriphenylphosphonium analogues. The most active analogues preferentially inhibited growth of *Mycobacterium tuberculosis* H37Rv (MIC<sub>50</sub> 2–4 μM) and were bactericidal against *Mycobacterium bovis* BCG (MBC<sub>99</sub> 3 μM). In spite of their propensity to accumulate within membranes, we found no evidence that these compounds permeabilized mycobacterial membranes or induced cell-envelope stress. Our investigations indicated that their bactericidal effects stem from sustained depolarization of mycobacterial membranes and ensuing disruptive effects on electron transfer and cell division.

**KEYWORDS:** Triphenylphosphonium cations, Cationic amphiphilic indoles, Antimycobacterial activity, Membrane depolarization



Tuberculosis (TB) poses an enduring threat to global health.<sup>1</sup> TB has consistently been ranked among the top ten causes of death worldwide since 2000.<sup>2</sup> Although incident TB rates have declined year on year, decreases have been incremental (1.5% from 2014 to 2015) and woefully short of the threshold levels of 4–5% annual reductions required to end the global TB epidemic.<sup>1</sup> A major impediment to effective TB control is the requirement for prolonged treatment with multiple drugs. Unless monitored closely, lapses in compliance are commonplace, and this in turn promotes the emergence of resistant strains of the causative organism *Mycobacterium tuberculosis*. The characteristically long treatment time of TB is attributed to “persister” bacteria that do not respond to standard drugs. Persons harboring these latent organisms, estimated at nearly one third of the global population, serve as silent reservoirs for transmission.<sup>3</sup> In order to improve the efficacy of TB treatment against mycobacterial persisters and drug-resistant organisms, novel antitubercular agents are urgently required.

Selective targeting of bacterial membranes has been mooted as a viable therapeutic strategy against infectious diseases.<sup>4</sup> The underpinning rationale is that a functionally intact cell membrane is mandatory for the survival of both replicating and dormant bacteria, including mycobacterial persisters. Perturbing the membrane would thus disrupt a multitude of embedded targets with lethal pleiotropic consequences, besides limiting the emergence of resistant strains.<sup>4</sup> The feasibility of this approach

is corroborated in several reports that have verified membrane disruption as causal to the antibacterial activity of structurally diverse compounds.<sup>5–8</sup> In spite of the chemical heterogeneity, these compounds are archetypal cationic amphiphiles, a motif which affords ready access to the lipophilic and negatively charged matrices of bacterial membranes.<sup>9</sup>

The triphenylphosphonium (TPP) cation is widely employed as a membrane-targeting motif.<sup>10,11</sup> Accumulation of TPP cations in polarized membranes is driven by their unique physicochemical properties (lipophilicity, large ionic radius, extensive charge delocalization) which secure enrichment by several hundred-fold in compartments with large negative membrane potentials ( $\Delta\psi$ ), such as the mitochondria (–170 mV), and most bacteria (–135 to –180 mV).<sup>10,12</sup> Indeed, conjugation of TPP to several mitochondrial-directed bioactive agents have led to significant gains in activity, conceivably due to enhanced localization within the mitochondria.<sup>10,13</sup> Separately, Dunn and co-workers reported remarkable increases in activity when TPP-pendant side chains were attached to antimycobacterial phenothiazines.<sup>14</sup> The authors contend that TPP served as a delivery vehicle, directing the phenothiazines to the mycobacte-

Received: July 18, 2017

Accepted: October 9, 2017

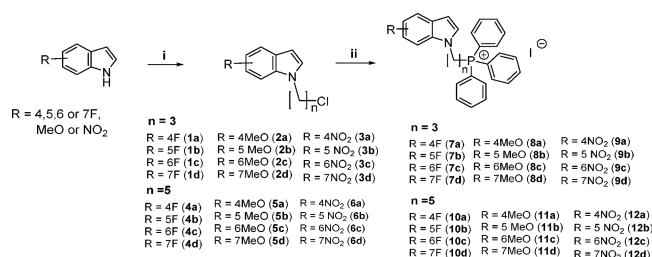
Published: October 9, 2017

rial membrane, thereby enhancing their inhibition of oxidative phosphorylation.

In a previous report, we described mycobactericidal cationic amphiphilic Mannich bases of 1-octylindoles which selectively disrupt mycobacterial membranes.<sup>7</sup> In an effort to explore the chemical diversity of indole-based cationic amphiphiles, we prepared indoles with alkyl TPP side chains. Unlike the aforementioned indole-based Mannich bases where charge and lipophilicity were segregated to distinct parts in the scaffold, both features are embedded within a single motif (TPP) in this series. We posited that these cationic amphiphilic indolylalkylTPP analogues would be membrane disrupting and, hence, mycobactericidal.

Our target compounds were synthesized by attaching the charged TPP headgroup to position 1 of 4-, 5-, 6-, and 7-fluoro/methoxy/nitroindoles via a three-carbon (propyl) or five-carbon (pentyl) linker (Scheme 1). The fluoro, methoxy, and nitro

**Scheme 1. Synthesis of Indolylalkyltriphenylphosphonium Analogues (7a–d to 12a–d) and Intermediates (1a–d to 6a–d)<sup>a</sup>**



<sup>a</sup>Reagents and conditions: (i) NaH, anhydrous DMF, 1-bromo-3-chloropropane or 1-bromo-5-chloropentane, 0 °C to rt; (ii) KI, triphenylphosphine, MeCN, reflux, 24–48 h.

groups were representative electron-donating (methoxy) and electron-withdrawing (fluoro, nitro) groups. The length of the alkyl linker did not exceed five-carbon to avoid excessive lipophilicity which was already high in the final compounds (clogP 8.6–9.8) (Table 1).

Synthesis of the TPP analogues was achieved by reacting the substituted indole with 1-bromo-3-chloropropane or 1-bromo-5-chloropentane in the presence of sodium hydride, after which the intermediates (1a–d to 6a–d) were reacted with triphenylphosphine and potassium iodide in refluxing acetonitrile for 24–48 h (Scheme 1). The mixture was then filtered, solvent was removed under reduced pressure, and desired products (7a–d to 12a–d) recrystallized (dichloromethane/ether) or purified by column chromatography if they were semisolids. Thereafter, they were evaluated for growth inhibition on *M. bovis* BCG, an attenuated tubercle bacillus and mycobacterial model organism, by the broth dilution method. Minimum inhibitory concentrations required to reduce bacterial growth by 50% (MIC<sub>50</sub>) and 90% (MIC<sub>90</sub>) were determined by turbidity measurements (Table 1).

As seen in Table 1, the propyl TPP indoles (7a–d to 9a–d) and pentyl TPP indoles (10a–d to 12a–d) inhibited bacterial growth over a comparatively narrow MIC<sub>50</sub> range (1–10 μM). Pentyl TPP analogues were generally more potent than their propyl TPP counterparts by 2-fold or more. Differential potencies among the fluoro, methoxy, and nitro regioisomers were not apparent, but there was some hint of regioselective preference for positions 4 and 7 among the methoxy- and nitro-

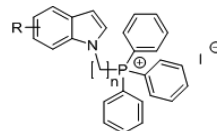
substituted analogues as seen from the greater potencies of 7-methoxy 11d, 4-nitro 12a, and 7-nitro 12d isomers.

Deconstruction of the scaffold revealed negligible activity in the component fragments, namely propyl TPP 13, pentyl TPP 14, and representative substituted indoles (5-fluoro-1-propyl-1H-indole 15, 7-methoxy-1-pentyl-1H-indole 16). A previous study on alkyl-TPP cations (C<sub>n</sub>H<sub>2n+1</sub>-TPP, where n = 4, 8, 10, or 12) found that only TPP cations with *n*-octyl and longer alkyl side chains significantly inhibited the growth of *Bacillus subtilis*.<sup>15</sup> Here we found the highly lipophilic *n*-decyl-TPP 17 to be as potent as several indolylalkyl TPP conjugates (Table 1). In fact, the antimycobacterial activities of these compounds (7a–d to 12a–d) were significantly correlated to lipophilicity (clogP) when analyzed by the nonparametric Spearman rank correlation statistical test (correlation coefficient of −0.562, p = 0.01, two-tailed, IBM-SPSS, Armonk, NY). This prompted us to question the role of the indole ring in our final compounds, namely if lipophilicity is its sole contribution to activity. To this end, a comparison of phenylhexyl TPP 18 and indolylpentyl TPP 19 proved insightful. The phenylhexyl side chain of 18 broadly resembles the ring-open fragment (phenyl-N-C<sub>5</sub>-) of the indolylpentyl moiety of 19. Both compounds had comparable MIC<sub>50</sub> values (Table 1) but the smaller difference in MIC<sub>50</sub> and MIC<sub>90</sub> of 19 (<2 fold) gave it a potency edge over 18. Several indolylpentyl TPPs (11d, 12a, 12c) demonstrated similar narrow differences in their MIC values, and while the reasons remain unclear, it is undoubtedly a desirable feature that may be associated with the indole ring.

We then selected two potent indolylpentyl TPPs—the methoxy analogue 11d and nitro analogue 12a—for further investigations (Table 2). Both 11d and 12a were similarly active against *M. tuberculosis* H37Rv. Encouragingly, they were also equally bactericidal, eradicating up to 99% of *M. bovis* BCG cultures at 3 μM. In terms of cytotoxicity, the compounds displayed a large selectivity advantage in terms of their minimal hemolytic activity on human red blood cells but a narrower 9-fold edge over mammalian Vero cells. The nitro analogue 12a was not genotoxic in the Ames test.<sup>16</sup> Compounds 8d and 9a, the propyl counterparts of 11d and 12a, were similarly investigated and, as anticipated, were less potent against *M. tuberculosis* H37Rv and exhibited weaker toxicity.

Next, we explored the membrane-perturbing properties of 11d and 12a. First, we monitored the melting profiles of dimyristoylphosphatidyl glycerol (DMPG) vesicles containing the test compound by differential scanning calorimetry (DSC). Negatively charged DMPG vesicles have been employed as surrogates of bacterial membranes.<sup>17</sup> Compound-induced disruption of the DMPG bilayers typically weakens interactions within the phospholipid array, leading to decreases in the gel to liquid melting temperature (*T*<sub>m</sub>) and diminished calorimetric enthalpy (Δ*H*) of the melting endotherm.<sup>18</sup> We found that both compounds caused only incremental losses to *T*<sub>m</sub> (~1 °C) and Δ*H* (~2-fold) of DMPG vesicles (Figure 1A). Propyl TPP (13) did not disrupt the DMPG melting endotherm, while the changes induced by the indole fragment 15 were comparable to those incurred by 11d and 12a. Collectively, these results pointed to minimal perturbation of the DMPG bilayers by 11d and 12a, which were no more pronounced than those caused by the inactive fragments 13 and 15.

While DMPG vesicles are acceptable mimics of the lipid membrane, they do not represent a real bacterial model. Thus, moving on, we treated *M. bovis* BCG cultures with 11d and 12a (2× MIC<sub>90</sub>) and monitored the uptake of propidium iodide (PI)

**Table 1. Antimycobacterial Activities (*M. bovis* BCG) and Estimated Lipophilicities (clogP) of Indolylalkyltriphenylphosphonium iodides (7a–d to 12a–d) and Related Analogues (13–19)**


| No | R                 | n=3                |                                       |                   | n=5                |                                       |                   |   |    |
|----|-------------------|--------------------|---------------------------------------|-------------------|--------------------|---------------------------------------|-------------------|---|----|
|    |                   | clogP <sup>a</sup> | <i>M. bovis</i> BCG (μM) <sup>b</sup> |                   | clogP <sup>a</sup> | <i>M. bovis</i> BCG (μM) <sup>b</sup> |                   |   |    |
|    |                   |                    | MIC <sub>50</sub>                     | MIC <sub>90</sub> |                    | MIC <sub>50</sub>                     | MIC <sub>90</sub> |   |    |
| 7a | 4-F               | 8.93               | 6                                     | 12                | 10a                | 4-F                                   | 9.81              | 3 | 5  |
| 7b | 5-F               | 8.93               | 8                                     | 17                | 10b                | 5-F                                   | 9.81              | 3 | 5  |
| 7c | 6-F               | 8.93               | 6                                     | 12                | 10c                | 6-F                                   | 9.81              | 3 | 5  |
| 7d | 7-F               | 8.93               | 5                                     | 12                | 10d                | 7-F                                   | 9.81              | 3 | 6  |
| 8a | 4-MeO             | 8.81               | 6                                     | 11                | 11a                | 4-MeO                                 | 9.68              | 3 | 5  |
| 8b | 5-MeO             | 8.81               | 10                                    | 23                | 11b                | 5-MeO                                 | 9.68              | 5 | 10 |
| 8c | 6-MeO             | 8.81               | 7                                     | 15                | 11c                | 6-MeO                                 | 9.68              | 4 | 8  |
| 8d | 7-MeO             | 8.81               | 4                                     | 6                 | 11d                | 7-MeO                                 | 9.68              | 2 | 3  |
| 9a | 4-NO <sub>2</sub> | 8.58               | 5                                     | 9                 | 12a                | 4-NO <sub>2</sub>                     | 9.46              | 2 | 3  |
| 9b | 5-NO <sub>2</sub> | 8.58               | 9                                     | 12                | 12b                | 5-NO <sub>2</sub>                     | 9.46              | 3 | 5  |
| 9c | 6-NO <sub>2</sub> | 8.58               | 7                                     | 13                | 12c                | 6-NO <sub>2</sub>                     | 9.46              | 3 | 4  |
| 9d | 7-NO <sub>2</sub> | 8.58               | 2                                     | 4                 | 12d                | 7-NO <sub>2</sub>                     | 9.46              | 1 | 2  |

|                                     | 13   | 14   | 15   | 16   | 17   | 18   | 19   |
|-------------------------------------|------|------|------|------|------|------|------|
| clogP <sup>a</sup>                  | 7.19 | 8.25 | 3.84 | 4.77 | 10.9 | 10.2 | 9.62 |
| MIC <sub>50</sub> (μM) <sup>b</sup> | >50  | 28   | >50  | >50  | 3.9  | 5.2  | 4.3  |
| MIC <sub>90</sub> (μM) <sup>b</sup> | >50  | >50  | >50  | >50  | 6.0  | 11.6 | 6.3  |

<sup>a</sup>Determined by ChemDraw Ultra Version 12.0.21076. <sup>b</sup>Minimum inhibitory concentrations required to reduce bacterial growth by 50% (MIC<sub>50</sub>) and 90% (MIC<sub>90</sub>) compared to untreated controls. Average of at least three separate determinations.

**Table 2. Mycobacterial and Cytotoxicity Profiles of Indolylpropyl-TTP (8d, 11d) and Indolylpentyl-TTP (9a, 12a) Analogues**

| no. | <i>M. tuberculosis</i> H37Rv <sup>a</sup> (μM) |                   | Vero IC <sub>50</sub> <sup>b</sup> (μM) | RBC HC <sub>50</sub> <sup>c</sup> (μM) | bactericidal activity <i>M. bovis</i> BCG (μM) <sup>d</sup> |                     |
|-----|------------------------------------------------|-------------------|-----------------------------------------|----------------------------------------|-------------------------------------------------------------|---------------------|
|     | MIC <sub>50</sub>                              | MIC <sub>90</sub> |                                         |                                        | MBC <sub>99</sub>                                           | MBC <sub>99.9</sub> |
| 8d  | 6                                              | 20                | 34                                      | >300                                   | 13                                                          | 25                  |
| 11d | 2                                              | 6                 | 18                                      | >300                                   | 3                                                           | 6                   |
| 9a  | 22                                             | 45                | >100                                    | 230                                    | 25                                                          | 50                  |
| 12a | 4                                              | 6                 | 36                                      | 196                                    | 3                                                           | 6                   |

<sup>a</sup>Minimum inhibitory concentrations required to reduce bacterial growth by 50% (MIC<sub>50</sub>) and 90% (MIC<sub>90</sub>) compared to untreated controls. <sup>b</sup>Concentration required to inhibit mammalian Vero cell viability by 50%, compared to untreated control cells. <sup>c</sup>Concentration required to lyse 50% of human RBC compared to positive control Triton-X 100 (2% v/v) which induced total hemolysis (100%). <sup>d</sup>Minimum bactericidal concentrations required to reduce initial number of colony forming units (CFU) by 99% (MBC<sub>99</sub>) and 99.9% (MBC<sub>99.9</sub>) compared to untreated controls. Average of two or more separate determinations.

by the treated cells over 1–5 days. PI is taken up exclusively by bacteria with permeabilized membranes where it binds to DNA and emits fluorescence. The intensity of the fluorescence is correlated to the proportion of cells with compromised membranes. The time-kill curves of 11d/12a-treated cultures were concurrently monitored to correlate changes in membrane integrity to cell viability. Controls were isoniazid which did not

permeabilize membranes and 20 (3-[[2,3-dihydrospiro(indene-1,4'-piperidin)-1'-yl]methyl]-6-methoxy-1-octyl-1H-indole), an antimycobacterial compound recently found by us to perturb bacterial membranes. As shown in Figure 1B,C, 11d and 12a, like isoniazid (Figure 1D), induced gradual increases in the proportion of cells with permeabilized membranes. These changes largely coincided with the bactericidal profiles of the compounds. In contrast, the permeabilization induced by 20 was rapid and observed before significant cell death had set in (Figure 1E).

The mycobacterial *iniBAC* gene cluster is involved in cell wall turnover, remodeling, or maintenance.<sup>19</sup> These genes are upregulated under conditions of cell envelope stress such as those encountered on exposure to cell wall inhibitors<sup>20</sup> or membrane-targeting cationic amphiphiles.<sup>7</sup> We were thus curious if the cationic amphiphilic 11d would induce transcriptional activity of the *iniBAC* cluster. To this end, we treated recombinant *M. bovis-piniBAC*-Red Fluorescent Protein (RFP) cultures with various concentrations (0.4–100 μM) of 11d or positive control isoniazid for 24 h. Induction would increase the fluorescent signal of the RFP whose coding sequence is controlled by the operon promoters. We found no induction of *iniBAC* activity by 11d in contrast to isoniazid, which duly increased activity (Supporting Information, Figure S1). Taken together, collateral evidence from the foregoing experiments did not support membrane disruption as causal to the antimycobacterial activities of the indolylpentyl TPPs.

Our initial hypothesis was that the intrinsic lipophilicities and charge-delocalized states of the indolylalkyl/TTP cations would promote their accumulation within the bacterial membrane.



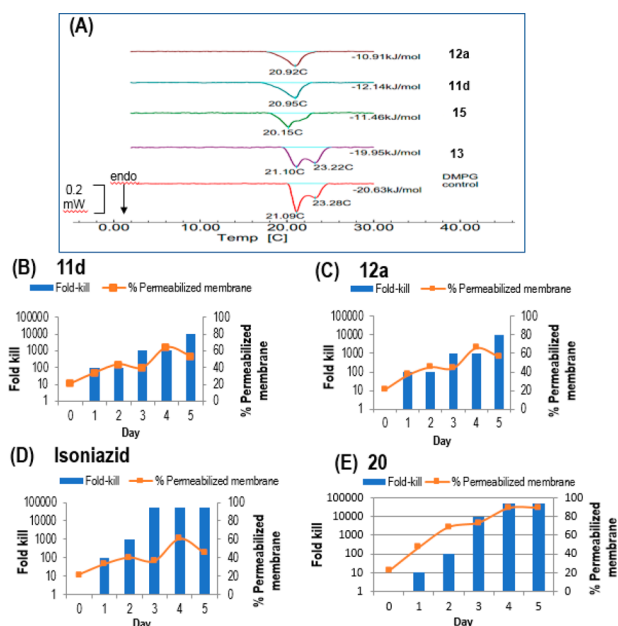


**Figure 1.** (A) Calorimetric curves in heating mode of DMPG vesicles containing 1 part test compound (**11d**, **12a**, **13**, and **15**) to 10 parts DMPG.  $T_m$  (°C) and  $\Delta H$  (kJ/mol) are indicated. Control DMPG vesicles showed a bifurcated endotherm with two  $T_m$  values.<sup>7</sup> (B–E) Percentage of permeabilized cells and fold-kill of *M. bovis* BCG cultures treated with test compounds over time.  $10^6$  CFU/mL mid log phase cultures were treated with  $2\times$  MIC<sub>90</sub> of (B) **11d** (6  $\mu$ M), (C) **12a** (6  $\mu$ M), (D) isoniazid (1.6  $\mu$ M), and (E) **20** (4  $\mu$ M). Samples were collected daily for determinations of CFU and % permeabilized bacteria compared to controls.

However, the preceding section has shown that the influx of these positively charged entities did not appear to have permeabilized bacterial membranes. We then asked if they could have disrupted the electrochemical gradient of the membrane as there is precedent of alkyl TPP cations ( $C_nH_{2n+1}^-$  TPP, where  $n = 4, 8, 10,$  or  $12$ ) depolarizing bacterial membranes with a rank order ( $C_{12} > C_{10} > C_8$ ) correlated to bactericidal activity.<sup>15</sup> Thus, we duly investigated the effects of **11d** and **12a** on the membrane potential of mycobacteria using the fluorescent membrane permeable dye 3,3-diethyloxycarbocyanine iodide (DiOC<sub>2</sub>) which selectively accumulates in bacterial cells with polarized membranes and emits red fluorescence. When exposed to nonviable cells into which it does not accumulate, DiOC<sub>2</sub> emits green fluorescence. Hence, the red/green fluorescence ratio of DiOC<sub>2</sub> provides a measure of cells with polarized membranes.

Here, we treated *M. bovis* BCG cultures with  $4\times$  MIC<sub>90</sub> of **11d** and **12a** and monitored the red/green ratio over time (20 min to 3 h). Interestingly, **11d** and **12a** caused a sharp drop in the ratio within 20 min, followed by gradual decreases which leveled off at 3 h (Figure 2A). At this point, the loss in membrane potential was comparable to that caused by the positive control CCCP. No change in the ratio was observed in cells treated with the fragments **14**, **16**, and the TB drug rifampicin, which was employed as a negative control. We then monitored the red/green ratios of **11d/12a** treated cells for longer periods (1, 3, 5 days) and found that they remained suppressed (Supporting Information, Figure S2). It is thus apparent that **11d** and **12a** induced a rapid and sustained loss in the membrane potential of treated mycobacteria. Tellingly, the early losses (by 20 min) were incurred prior to the onset of significant cidal activity (Figure

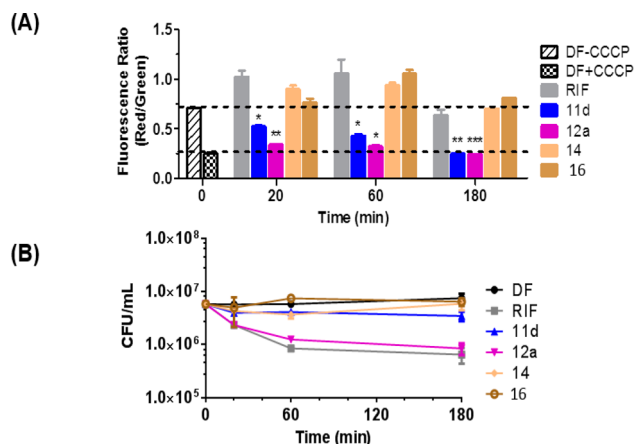


**Figure 2.** (A) Changes in membrane potential (red/green fluorescent ratio of DiOC<sub>2</sub>) of *M. bovis* BCG cultures treated with test compound **11d** (12  $\mu$ M), **12a** (24  $\mu$ M), **14** (24  $\mu$ M), **16** (24  $\mu$ M), rifampicin (RIF, 0.08  $\mu$ M), and CCCP (100  $\mu$ M). **11d** and **12a** were tested at  $4\times$  MIC<sub>90</sub>. MIC<sub>90</sub> was redetermined for this experiment and were 3  $\mu$ M (**11d**) and 6  $\mu$ M (**12a**). Mean and SD of three biological replicates. Means were significantly different from drug-free (DF) controls at time zero (without CCCP) with  $p < 0.05$  (\*),  $< 0.01$  (\*\*), and  $< 0.001$  (\*\*\*) (Student's  $t$  test, Graph-Pad Prism, Ver 5.0). (B) Corresponding changes in viability of treated cultures (CFU/mL) under similar conditions described in (A).

2B), thus implicating a bonafide depolarizing action by the test compounds.

Dissipation of the membrane potential has been reported to disrupt the organized distribution of cell division-related and cytoskeletal proteins in bacteria.<sup>21</sup> The loss in spatial localization of these proteins has striking consequential effects on bacterial morphology, as reported for several depolarizing antibiotics.<sup>22,23</sup> We were thus curious if the membrane-depolarizing effects of **11d** and **12a** would induce morphological changes in mycobacteria. To this end, *M. bovis* BCG cultures were microscopically examined after incubation with **11d** and **12a** at their MIC<sub>90</sub> for 1, 3, and 5 days. We observed distinct elongation of treated cells (Supporting Information, Figure S3) which suggests defective septum formation during the cell division process. It is tempting to associate these morphological aberrations to the loss in membrane potential induced by **11d** and **12a**.

The membrane potential affects energy production within the cell through its intimate links with the electron-transport chain (ETC). Electron transport in mycobacteria is initiated by the activity of various dehydrogenases (NADH dehydrogenase, succinate dehydrogenase) which transfer electrons sequentially from reduced nucleotides to the lipophilic redox carrier menaquinone and then to various cytochrome oxidases.<sup>24</sup> It is beyond the scope of this report to interrogate the effects of **11d** and **12a** on the different components of the ETC. However, to obtain a sense of whether the ETC is implicated, two experiments were planned.

First, we assessed the effects of **11d** and **12a** on the reduction of the tetrazolium dye MTT. In viable cells, MTT is reduced to purple formazan crystals in a reaction mediated by dehydrogenases and coupled to electron transfer from reduced nucleotides. Broadly, this reduction reflects unimpeded electron flow and, by extension, electron transport efficiency in the bacilli.<sup>19</sup> If electron transfer is intercepted in any way, limited or no reduction of MTT will occur. Here, we treated *M. bovis* BCG

cultures with various concentrations (0.2–100  $\mu\text{M}$ ) of **11d** and **12a** for 30 min and 1 h, after which MTT was added and the production of the purple formazan reduction product monitored at 595 nm. Figure 3 shows that both compounds caused

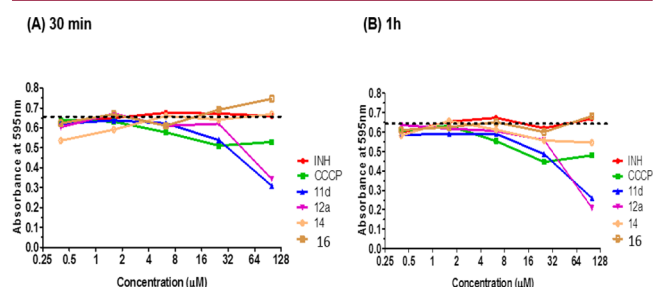


**Figure 3.** Reduction of tetrazolium dye MTT to formazan by *M. bovis* BCG cultures treated for (A) 30 min and (B) 1 h at various concentrations of **11d**, **12a**, **14**, and **16**, isoniazid (INH), and ionophore CCCP (positive control, 100  $\mu\text{M}$ ). Dashed line indicates the basal absorbance of formazan (595 nm) in drug-free cultures. Diminished reduction of MTT results in less formazan being formed (decrease in absorbance). Results shown are representative of two independent experiments.

concentration (but not time) dependent losses in formazan formation. At the highest test concentration of 100  $\mu\text{M}$ , formazan production was diminished by half, exceeding that caused by the positive control CCCP. Isoniazid and the inactive fragments (**14**, **16**) did not affect MTT reduction. Thus, the rapid depolarizing effects of **11d** and **12a** adversely affected the reductive capacity of the mycobacteria.

Next, we performed methylene blue decolorization assays to assess oxygen uptake in **11d/12a**-treated *M. bovis* BCG. Decolorization of methylene blue indicates utilization of oxygen and a functional respiratory chain in bacteria.<sup>19</sup> Briefly, bacterial cultures were exposed to **11d** or **12a** at 5 $\times$ , 10 $\times$ , and 15 $\times$  MIC<sub>90</sub> for 1 h, followed by addition of methylene blue and incubation in an oxygen-free environment for 12 h. In order to account for toxic effects which would be apparent at these high doses, we assessed the viability of the treated cultures postincubation by enumerating their colony-forming capacities.

Figure 4A shows that the positive control thioridazine, an inhibitor of Type II NADH dehydrogenase (NDH2) in the ETC, did not decolorize methylene blue. On the other hand, decolorization was observed in cultures treated with the fragments **14** and **16** which did not cause membrane depolarization (Supporting Information, Figure S4). We found that **11d** and **12a** decolorized methylene blue at 5 $\times$  MIC<sub>90</sub> but not at higher concentrations (Figure 4B, C). However, the results obtained at 15 $\times$  MIC<sub>90</sub> were discounted due to the confounding effects of cell death observed at this concentration. In contrast, cultures treated with 10 $\times$  MIC<sub>90</sub> **11d** or **12a** had CFU levels that were comparable to those observed at 5 $\times$  MIC<sub>90</sub>. The viability of these cultures coupled with the absence of methylene blue decolorization led us to conclude that **11d** and **12a** inhibited oxygen consumption under these conditions. In summary, the ability of **11d** and **12a** to induce membrane depolarization, impair reductive capacity, and diminish respiration in *M. bovis* BCG cultures are indicative of their disruptive effects on electron transport and energy production by the bacilli.

Few antimicrobial TPP derivatives have been reported to date.<sup>14,25,26</sup> However, the unique ability of the phosphonium cation to hone in to negatively charged cellular compartments

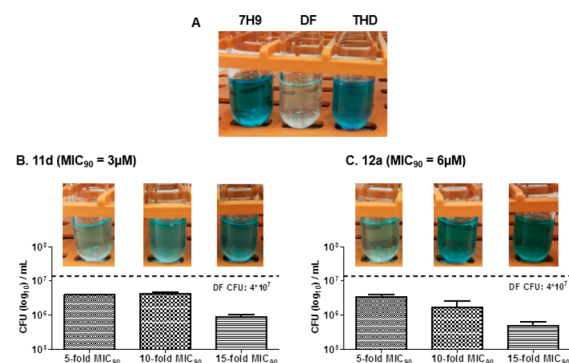


**Figure 4.** Oxygen consumption of 0.001% methylene blue containing *M. bovis* BCG cultures. (A) Control tubes containing methylene blue and 7H9 medium (7H9) only, medium and mid log phase *M. bovis* BCG without test compound (DF) and containing positive control thioridazine THD (80  $\mu\text{M}$ ). Cultures were incubated at 37  $^{\circ}\text{C}$ , 12 h. (B) *M. bovis* BCG cultures (mid log phase) containing methylene blue treated with **11d** at 5 $\times$  (15  $\mu\text{M}$ ), 10 $\times$  (30  $\mu\text{M}$ ), and 15 $\times$  (45  $\mu\text{M}$ ) MIC<sub>90</sub>. Cultures were incubated at 37  $^{\circ}\text{C}$ , 12 h. CFU determinations were carried out post incubation on each **11d**-treated culture to determine cell viability. (C) As in (B) except that cultures were treated with **12a** at 5 $\times$  (30  $\mu\text{M}$ ), 10 $\times$  (60  $\mu\text{M}$ ), and 15 $\times$  (90  $\mu\text{M}$ ) MIC<sub>90</sub>.

such as bacterial membranes or the mitochondria of parasites, which are critical for survivability, provides an unrivaled opportunity at selective targeting. We have shown here that grafting a phosphonium headgroup onto an otherwise inert substituted indole scaffold sharply increased antimycobacterial potencies by 10-fold or more. The improvement in potency was largely driven by gains in lipophilicity brought about by the conjugation. By extrapolation, this should also augment the ability of the phosphonium analogues to accumulate within the mycobacterial membrane. That the influx of these cations into the membranous matrix did not result in an overt loss of membrane integrity was thus a surprise. The potent analogues (**11d**, **12a**) did not perturb the melting behavior of phospholipid vesicles, showed no evidence of permeabilizing mycobacterial membranes, and did not increase transcriptional competency of the *iniBAC* gene cluster as would be expected if the membrane was subjected to stress. Rather, what emerged was a significant loss in the membrane potential of **11d/12a**-treated mycobacteria which was incurred within 20 min of exposure and persisted up to 24 h and longer. We posit that collateral damage to the bacterium arising from aberrations to the membrane potential, such as disrupted electron transfer in the ETC (as seen from the MTT and oxygen consumption assays) and abnormal cell division, were the ultimate mediators of compound-induced toxicity. In conclusion, our findings demonstrate the potential of phosphonium derivatives as antimycobacterial agents that act via membrane depolarization.

## ■ ASSOCIATED CONTENT

### Supporting Information

The Supporting Information is available free of charge on the ACS Publications website at DOI: 10.1021/acsmchemlett.7b00287.

Description of methods employed in the synthesis of intermediates and final compounds; experimental details; Figures S1–S4 (PDF)

## AUTHOR INFORMATION

### Corresponding Author

\*E-mail: [phagoml@nus.edu.sg](mailto:phagoml@nus.edu.sg).

### ORCID

Thomas Dick: 0000-0002-9604-9452

Mei-Lin Go: 0000-0003-4757-3343

### Author Contributions

The manuscript was written through contributions of all authors. M.L. and S.A.N. contributed equally.

### Notes

The authors declare no competing financial interest.

<sup>†</sup>Joint first authors.

## ACKNOWLEDGMENTS

The authors acknowledge support from the Singapore Ministry of Health National Medical Research Council TCR Flagship grant NMRC/TCR/011-NUHS/2014 and Centre Grant "MINE", Research Core #4 NMRC/CG/013/2013 to T.D., Ministry of Education Academic Research Fund R148000234114 to M.-L.G., and graduate scholarships to M.L., S.A.N. This work is part of the Singapore Program of Research Investigating New Approaches to Treatment of Tuberculosis (SPRINT TB) led by Dr N. Paton of National University of Singapore (NUS). We thank S. Phyu, M. Gengenbacher and Low J.L. of NUS for BSL3 core and lab management support. Dr. D. Alland (Rutgers University, New Jersey Medical School) for the *piniBAC* reporter plasmid, and Dr. Y. Yamada (NUS) for providing a modified version of the *M. bovis* BCG-*piniBAC*-RFP strain.

## ABBREVIATIONS

BCG, Bacillus Calmette-Guerin; CCCP, carbonyl cyanide *m*-chlorophenyl hydrazone; DiOC<sub>2</sub>, 3,3'-diethyloxycarbocyanine iodide; Log *P*, logarithm to base 10 of partition coefficient *P*; MTT, 3-(4,5-dimethylthiazol-2-yl)-2,5-diphenyltetrazolium bromide; PI, propidium iodide; RFP, red fluorescent protein; TPP, triphenylphosphonium

## REFERENCES

- (1) World Health Organization. *Global tuberculosis report 2016*; WHO Press: Paris, 2016.
- (2) World Health Organization. *Media Centre Fact Sheet, The Top 10 Causes of Death*, <http://www.who.int/mediacentre/factsheets/fs310/en/> (accessed January 2017).
- (3) World Health Organization, Media centre Fact sheet, *Tuberculosis*, <http://www.who.int/mediacentre/factsheets/fs104/en/> (accessed March 2017).
- (4) Hurdle, J. G.; O'Neill, A. J.; Chopra, I.; Lee, R. E. Targeting bacterial membrane function: an underexploited mechanism for treating persistent infections. *Nat. Rev. Microbiol.* **2011**, *9*, 62.
- (5) Koh, J. J.; Zou, H.; Mukherjee, D.; Lin, S.; Lim, F.; Tan, J. K.; Tan, D. Z.; Stocker, B. L.; Timmer, M. S. M.; Corkran, H. M.; Lakshminarayanan, R.; Tan, D. T. H.; Cao, D.; Beuerman, R. W.; Dick, T.; Liu, S. Amphiphilic Xanthenes as a Potent Chemical Entity of Anti-microbial Agents with Membrane-Targeting Properties. *Eur. J. Med. Chem.* **2016**, *123*, 684.
- (6) Moreira, W.; Aziz, D.; Dick, T. Boromycin kills mycobacterial persisters without detectable resistance. *Front. Microbiol.* **2016**, *7*, 199 DOI: 10.3389/fmicb.2016.00199.
- (7) Yang, T. M.; Moreira, W.; Nyantakyi, S. A.; Chen, H.; Aziz, D.; Go, M. L.; Dick, T. Amphiphilic indole derivatives as antimycobacterial agents: Structure-Activity Relationships and Membrane Targeting Properties. *J. Med. Chem.* **2017**, *60*, 2745.

(8) Wang, B.; Pachaiyappan, B.; Gruber, J. D.; Schmidt, M. G.; Zhang, Y.; Woster, P. M. Antibacterial diamines targeting bacterial membranes. *J. Med. Chem.* **2016**, *59*, 3140.

(9) Yeaman, M. R.; Yount, N. Y. Mechanisms of antimicrobial peptide action and resistance. *Pharmacol. Rev.* **2003**, *55*, 27.

(10) Madak, J. T.; Neamati, N. Membrane Permeable Lipophilic Cations as Mitochondrial Directing Groups. *Curr. Top. Med. Chem.* **2015**, *15*, 745.

(11) Ross, M. F.; Prime, T. A.; Abakumova, I.; James, A. M.; Porteous, C. M.; Smith, R. A. J.; Murphy, M. P. Rapid and extensive uptake and activation of hydrophobic triphenylphosphonium cations within cells. *Biochem. J.* **2008**, *411*, 633.

(12) Krulwich, T. A.; Sachs, G.; Padan, E. Molecular Aspects of Bacterial pH Sensing and Homeostasis. *Nat. Rev. Microbiol.* **2011**, *9*, 330.

(13) Yousif, L. F.; Stewart, K. M.; Kelley, S. O. Targeting mitochondria with organelle-specific compounds: Strategies and applications. *ChemBioChem* **2009**, *10*, 1939.

(14) Dunn, E. A.; Roxburgh, M.; Larsen, L.; Smith, R. A. J.; McLellan, A. D.; Heikal, A.; Murphy, M. P.; Cook, G. M. Incorporation of triphenylphosphonium functionality improves the inhibitory properties of phenothiazine derivatives in *Mycobacterium tuberculosis*. *Bioorg. Med. Chem.* **2014**, *22*, 5320.

(15) Khailova, L. S.; Nazarov, P. A.; Sumbatyan, N. V.; Korshunova, G. A.; Rokitskaya, T. I.; Dedukhova, V. I.; Antonenko, Y. N.; Shulachev, V. P. Uncoupling and Toxic Action of Alkyltriphenylphosphonium Cations on Mitochondria and the Bacterium *Bacillus subtilis* as a Function of Alkyl Chain Length. *Biochemistry (Moscow)* **2015**, *80*, 1589.

(16) McCann, J.; Choi, E.; Yamasaki, E.; Ames, B. N. Detection of Carcinogens as Mutagens in the Salmonella/microsome Test: Assay of 300 Chemicals. *Proc. Natl. Acad. Sci. U. S. A.* **1975**, *72*, 5135.

(17) Pinheiro, M.; Arede, M.; Nunes, C.; Caio, J. M.; Moiteiro, C.; Lucio, M.; Reis, S. Differential interactions of rifabutin with human and bacterial membranes: implication for its therapeutic and toxic effects. *J. Med. Chem.* **2013**, *56*, 417.

(18) Seydel, J. K. Analytical Tools for the Analysis and Quantification of Drug-Membrane Interactions. In *Drug-membrane interactions: analysis, drug distribution, modeling*; Seydel, J. K., Wiese, M., Eds.; Wiley-VCH: Weinheim, 2002; pp 51–139.

(19) Boshoff, H. I. M.; Myers, T. G.; Copp, B. R.; McNeil, M. R.; Wilson, M. A.; Barry, C. E., III The Transcriptional Responses of *Mycobacterium tuberculosis* to Inhibitors of Metabolism. *J. Biol. Chem.* **2004**, *279*, 40174.

(20) Alland, D.; Steyn, A. J.; Weisbrod, A. J.; Aldrich, K.; Jacobs, W. R., Jr. Characterization of the *Mycobacterium tuberculosis iniBAC* promoter, a promoter that responds to cell wall biosynthesis inhibition. *J. Bacteriol.* **2000**, *182*, 1802.

(21) Strahl, H.; Hamoen, L. W. Membrane Potential is Important for Bacterial Cell Division. *Proc. Natl. Acad. Sci. U. S. A.* **2010**, *107*, 12281.

(22) Hyde, A. J.; Parisot, J.; McNichol, A.; Bonev, B. B. Nisin-induced changes in *Bacillus* morphology suggest a paradigm of antibiotic action. *Proc. Natl. Acad. Sci. U. S. A.* **2006**, *103*, 19896.

(23) Beven, L.; Wroblewski, H. Effect of natural amphipathic peptides on viability, membrane potential, cell shape and motility of mollicutes. *Res. Microbiol.* **1997**, *148*, 163.

(24) Black, P. A.; Warren, R. M.; Louw, G. E.; van Helden, P. D.; Victor, T. C.; Kana, B. D. Energy Metabolism and Drug Efflux in *Mycobacterium tuberculosis*. *Antimicrob. Agents Chemother.* **2014**, *58*, 2491.

(25) Long, T. E.; Lu, X.; Galizzi, M.; Docampo, R.; Gut, J.; Rosenthal, P. J. Phosphonium Lipocations as Agents. *Bioorg. Med. Chem. Lett.* **2012**, *22*, 2976.

(26) Ke, H.; Morrisey, J. M.; Qu, S.; Chantarasriwong, O.; Mather, M. W.; Theodorakis, E. A.; Vaidya, A. B. Caged Garcinia Xanthenes, a Novel Chemical Scaffold with Potent Antimalarial Activity. *Antimicrob. Agents Chemother.* **2017**, *61*, e01220-16.